ISA
TRANSACTIONS®

ISA Transactions 44 (2005) 329–343

Modeling supply and return line dynamics for an electrohydraulic actuation system

Beshahwired Ayalew* Bohdan T. Kulakowski†

The Pennsylvania Transportation Institute, 201 Transportation Research Building, University Park, PA 16802, USA

(Received 30 June 2004; accepted 6 December 2004)

Abstract

This paper presents a model of an electrohydraulic fatigue testing system that emphasizes components upstream of the servovalve and actuator. Experiments showed that there are significant supply and return pressure fluctuations at the respective ports of the servovalve. The model presented allows prediction of these fluctuations in the time domain in a modular manner. An assessment of design changes was done to improve test system bandwidth by eliminating the pressure dynamics due to the flexibility and inertia in hydraulic hoses. The model offers a simpler alternative to direct numerical solutions of the governing equations and is particularly suited for control-oriented transmission line modeling in the time domain. © 2005 ISA—The Instrumentation, Systems, and Automation Society.

Keywords: Hydraulic system modeling; Supply and return line dynamics; Accumulator model; Hydraulic hoses; Modal approximation

1. Introduction

A very common assumption in the development of models for valve-controlled hydraulic actuation systems is that of constant supply and return pressures at the servovalve [1–4]. On the other hand, a survey of work on fluid transmission line dynamics suggests that significant pressure dynamics are introduced in hydraulic systems as a result of the compressibility and inertia of the oil as well as the flexibility of the oil and the walls of pipelines [5–8]. Transmission line dynamics can be significant on the supply and return lines between the hydraulic power unit (pump) and the servovalve as well as between the servovalve and the actuator manifold.

Close-coupling (i.e., mounting the servovalve directly on the actuator manifold) is often used as a solution to the problem of minimizing the effects of transmission line dynamics between the servovalve and the ports of short-stroke actuators. In the case of long-stroke actuators, where close coupling may not be physically feasible, the effect of transmission line dynamics can be analyzed by explicitly including a transmission line model in the model of the servosystem, as shown by Van Schothorst [9]. However, in the case of the supply line to the servovalve, close coupling may not be a convenient solution for either short- or long-stroke actuators, since usually the hydraulic power supply (HPS) unit, including the hydraulic pump, drive unit, heat exchangers, and cooling water pumps, needs to be housed separately, away from the work station of the actuator or the load frame supporting the actuator. In such cases, supply and return lines from the HPS to the servovalve that are of significant length may be unavoidable. In addition, from installation considerations, these

*Corresponding author. Tel.: (814) 863-8057; fax: (814) 865-3039. *E-mail address*: beshah@psu.edu

†Tel.: (814) 863-1893; fax: (814) 865-3039. *E-mail address*: btkl@psu.edu

Nomenclature

A_b, A_t	piston areas for the bottom and top chambers, respectively
A_i, B_i, C_i	feedback, input and output matrices, respectively, in modal state equation, Eq. (8)
c_{di}	discharge coefficient
c_s	experimental friction parameter for Eq. (26)
d	diameter of line section
$F_c^{\pm}$	sign-dependent Coulomb friction
F_{ext}	external force on piston not including gravity and friction
F_f	friction force on piston
$F_s^{\pm}$	sign-dependent static friction force
$Fv^{\pm}$	sign-dependent viscous friction coefficient
G	steady-state correction matrix given by Eq. (14)
G_v	gain of valve in Eq. (22)
I_2	identity matrix of size 2
i	mode index
i_v	servovalve current
$K_{v,i}$, K_v	valve coefficients given by, Eqs. (20) and (21)
L	length of line section
m	polytropic exponent
m_p	lumped mass of piston, fixture, and oil mass in cylinder
n	number of modes retained in approximation
p_a, q_a	oil side pressure and flow rate into the accumulator
p_b, p_t	pressure in the bottom and top cylinder chambers
p_d, q_d	downstream pressure and flow rate for a line section
P_d, Q_d	Laplace domain downstream pressure and flow rate
p_{di}, q_{ui}	downstream pressure and upstream flow rate as modal states in Eq. (8)
p_g	gas pressure in accumulator
p_{g0}	initial gas pressure
p_R	return pressure at servovalve
p_S	supply pressure at servovalve
p_u, q_u	upstream pressure and flow rate for a line section
P_u, Q_u	Laplace domain upstream pressure and flow rate
q	flow rate
q_b, q_t	flow to the bottom and from the top cylinder chamber
$q_{e,b}$, $q_{e,t}$	external leakage from bottom and top chambers
q_i	internal leakage in cylinder
Q_N	rated servovalve flow rate
R_{HSM}	linearized hydraulic resistance for the hydraulic service manifold
s	Laplace operator
u_1, u_2, u_3, u_4	underlap or overlap lengths for servovalve spool
V_b, V_t	bottom and top cylinder chamber volumes
V_g	instantaneous gas volume in accumulator
V_{g0}	initial gas volume in accumulator
v_p	piston velocity
w_i	port widths
x_p	piston position
x_v	servovalve spool displacement
$x_{v\,\max}$	maximum spool displacement
Z_c	line characteristic impedance
Z_0	line impedance constant
α, β	frequency-dependent viscosity correction factors
β_c, β_e	effective bulk modulus for cylinder chamber and transmission line
Γ	propagation operator
Δp_{HSM}	pressure drop across the hydraulic service manifold
Δp_N	rated pressure drop in servovalve specification
ρ	density of hydraulic oil
ν	kinematic viscosity of oil
ω	frequency in rad/s
ω_c	viscosity frequency, $\omega_c = \nu/r_h^2$
ω_{ci}	modal undamped natural frequencies of blocked line given by Eq. (9)
ω_n	natural frequency for valve model
ζ	damping ratio for valve model

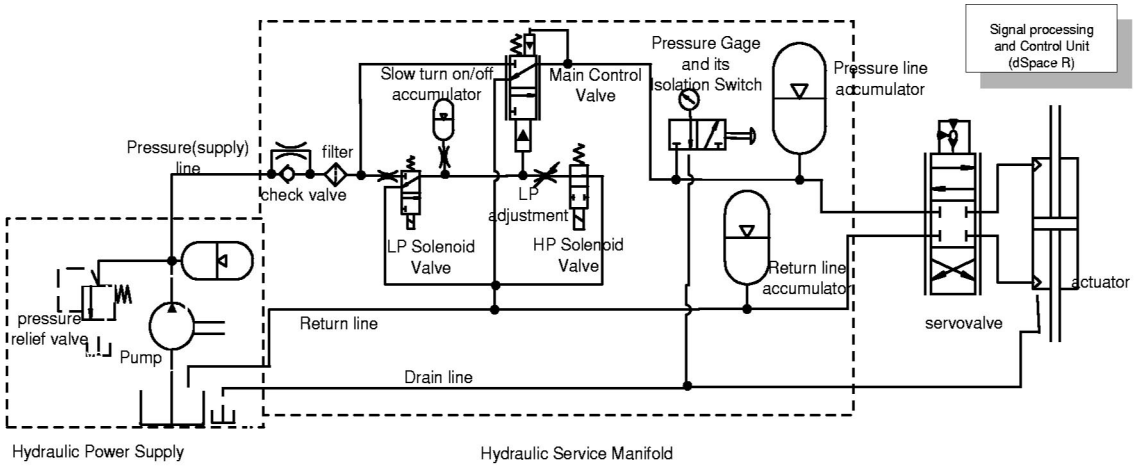

Fig. 1. Schematic of test system (HP=high pressure, LP=low pressure).

supply and return lines are usually flexible hoses rated for the appropriate working pressure.

Aside from the extensive presentation by Viersma [7], not much has been reported on the analysis of a hydraulic servosystem including supply pressure variations at the servovalve. Viersma's analysis was done in the frequency domain and the emphasis was to provide design rules for the location and sizing of the components of hydraulic servosystems. Yang and Tobler [10] developed a modal approximation technique that enables analysis of fluid transmission lines in the time domain via state space formulations. Modal approximation results provide modular and simpler alternatives to direct numerical time-domain solutions of the flow equations.

In this paper, the authors present and use modal approximation results within a model of an electrohydraulic actuation system to investigate supply and return pressure variations at the servovalve due to transmission line dynamics. Open-loop and closed-loop tests were conducted to validate the model. The model was then used to make a quick evaluation of alternative layouts of the supply and return lines.

2. Description of test system

The hydraulic system shown schematically in Fig. 1 was designed for fatigue testing applications. The servovalve is a 5-gpm (19 lpm) two-stage servovalve employing a torque motor driven double nozzle-flapper first stage and a main spool output stage. The servovalve is close coupled with a 10-kN, 102-mm-stroke symmetric actuator, which is mounted on a load frame. Pressure transducers are used for sensing the pressures at the four ports of the servovalve. A linear variable differential transformer (LVDT) is mounted on the actuator piston for position measurement.

Control and signal processing is done with a dSpace® 1104 single processor board, which includes onboard A/D and D/A converters and a slave digital signal processor (DSP). An amplifier circuit converts a 0–10-V control output from the dSpace® D/A to a high-impedance ±50-mA current input to the torque motor coils of the servovalve.

The unit labeled hydraulic services manifold (HSM) is connected to the servovalve using 3.048-m-long SAE-100R2 hoses. The hydraulic power supply (HPS) unit, including its heat exchanger and drive units, is housed separately and is connected to the HSM via 3.048-m-long SAE-100R2 hoses. The HSM provides basic line pressure regulation via the accumulators. In addition, the HSM is equipped with a control manifold circuitry to permit selection of high- and low-pressure operating modes, low-pressure level adjustment, slow pressure turn-on and turn-off, and fast pressure unloading. The drain line provides a path for oil that seeps past the seals in the actuator and also for draining oil from the HSM pressure gage.

During a normal fatigue testing operation, both the low-pressure and high-pressure solenoids are energized, the main control valve is completely

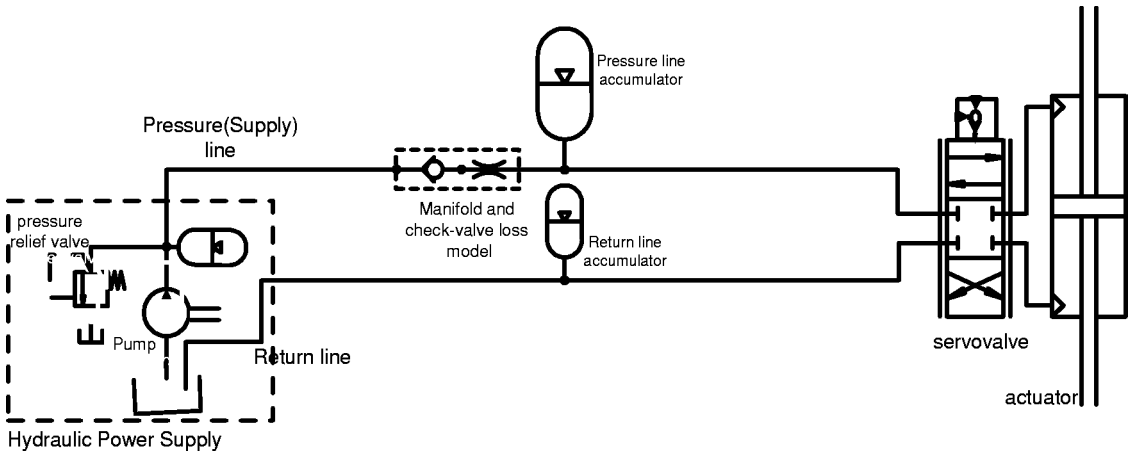

Fig. 2. Simplified system.

wide open, and the circuitry of the HSM allows flow at full system pressure [11]. We therefore model the HSM by considering the lumped nonlinear resistance arising from change of flow directions, flow cross sections, as well as flow in the filter element. The total pressure drop between the pressure inlet and outlet ports of the HSM is given in manufacturer specifications. The available data satisfy a nonlinear expression relating flow rate to pressure drop. While the HSM unit is rated for a wide range of flow rate capacities, the rated flow rate through the servovalve is within 10% of nominal flow rate of the HSM. We therefore use a local linear approximation to account for losses in the HSM,

$$\Delta p_{HSM} = R_{HSM} q. \tag{1}$$

We further assume that the check valve is an ideal one, so that its own dynamics are fast enough to be neglected and its backflow restriction has a large enough parallel resistance that the permitted backflow is very small. We also consider the drain flow to be negligible. With these simplifications, the system reduces to the one shown in Fig. 2. It should be noted that the resistances were lumped in the HSM excluding the gas-charged accumulators.

We make one more assumption before we proceed. Through extensive frequency domain analysis, Viersma [7] has shown that, provided that the accumulator and the pressure relief valve on the hydraulic power supply unit are located sufficiently close to the pump outlet (within 0.3 m), the pump flow pulsation frequencies can be suppressed from the pump output pressure. Therefore, in the following analysis, it is assumed that the output pressure just after the accumulator and pressure relief valve connection points in the HPS unit can be set as a known pressure input to the rest of the system. In fact, this is not a very restrictive assumption, since the modeling approach presented here is modular and models of the upstream components of the whole HPS unit can be incorporated if needed.

For the simplified system, we now have two sections of transmission hoses to model. The first section is for the supply and return hoses between the HPS and the HSM and the second is for the hoses between the HSM and the servovalve. A model applicable for each section is discussed next.

3. Model of transmission lines

To model the hydraulic hoses for our system, we refer to previous rigorous results on validated solutions of the mass and momentum conservation equations governing flow in one-dimensional fluid transmission lines having a circular cross section [5,6,8]. In general, some assumptions are necessary for the basic results to hold. These assumptions include laminar flow in the lines, negligible gravitational effects, negligible tangential velocity, and negligible variations of pressure and density in the radial and tangential directions. We also assume constant and uniform temperature and ignore heat transfer effects in the fluid line. We thereby limit the discussion to the linear friction model, which does not include distributed viscosity and

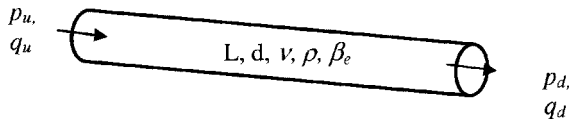

Fig. 3. A fluid transmission line.

heat transfer effects [6,10]. Corrections are applied to account for the frequency dependence of viscosity on the linear friction model, following the work of Yang and Tobler [10].

The flow lines are assumed to have rigid walls in some derivations [1,7]. However, Blackburn *et al.* [12] and McCloy and Martin [13] arrive at the same governing equations as the rigid wall case (for a frictionless flow) by allowing for wall flexibility and defining an effective bulk modulus combining the flexibility of the wall and that of the oil. Their definition of effective bulk modulus is the same as that derived by Merritt [4], where the effective bulk modulus is viewed as a series interconnection of the ''stiffness'' of the oil, of a container wall and even of entrapped air volume in the oil. Following this approach, we consider flexibility effects via the effective bulk modulus β_e. The model parameters required for any section of the transmission line reduce to the ones shown in Fig. 3. For the hydraulic hoses in this work, nominal values of the bulk modulus were taken from Ref. [13].

Using the above assumptions for the single transmission line, the conservation laws can be integrated in the Laplace domain to yield a well-known distributed parameter model commonly expressed as a two-port matrix equation and sometimes known as the four-pole equation [1,7]. The four-pole equations can take four physically realizable causal forms [6,9,12]. Two of these four are readily relevant to the problem at hand: one for the supply line hoses and another one for the return line hoses. The third one also finds use with accumulator connection lines, as discussed by Ayalew and Kulakowski [14].

Taking the supply line case first, we notice that in most hydraulic servosystem applications, a control signal modulates the servovalve consumption flow rate downstream of the supply line, $q_d(t)$, following the excursions of the (loaded) actuator piston. Then $q_d(t)$ is a preferred input to the transmission line model, and a realizable causality form requires that either $p_u(t)$ or $q_u(t)$ should be the other input [12]. Since we have already assumed the pressure just after the connection point of the pressure relief valve and first accumulator to be taken as an input to the system, the desired causal form of the four-pole equations for the supply line is the so-called pressure-input/pressure-output causality form [15]. It can be derived by defining the boundary conditions for the distributed parameter model as the upstream pressure and flow rate (p_u, q_d) and the downstream pressure and flow rate (p_d, q_u) at the opposite ends of the line,

$$\begin{bmatrix} P_d(s) \\ Q_u(s) \end{bmatrix} = \begin{bmatrix} \dfrac{1}{\cosh\Gamma(s)} & -\dfrac{Z_c(s)\sinh\Gamma(s)}{\cosh\Gamma(s)} \\ \dfrac{\sinh\Gamma(s)}{Z_c(s)\cosh\Gamma(s)} & \dfrac{1}{\cosh\Gamma(s)} \end{bmatrix} \times \begin{bmatrix} P_u(s) \\ Q_d(s) \end{bmatrix}. \tag{2}$$

The definitions of the propagation operator $\Gamma(s)$ and the line characteristic impedance $Z_c(s)$ depend on the friction model chosen [6,9]. In this paper, the authors use the approach of Yang and Tobler [10] that incorporated frequency-dependent damping and natural frequency modification factors into analytically derived modal representations of the four-pole equations for the linear friction model. $\Gamma(s)$ and $Z_c(s)$ are defined by

$$\Gamma(s) = D_n \frac{d^2 s}{4\nu} \sqrt{\alpha^2 + \frac{32\alpha\beta\nu}{sd^2}}, \tag{3}$$

$$Z_c(s) = Z_0 \sqrt{\frac{32\alpha\beta\nu}{sd^2} + \alpha^2}. \tag{4}$$

The frequency-dependent correction factors α and β are obtained by comparing the modal undamped natural frequencies and damping coefficients of the modal approximations of the dissipative (''exact'') model, which is described in detail in Ref. [16], against the modal representation of the linear friction model [10]. Corrected kinematic viscosity (ν) values are used [8]. The dimensionless numbers D_n and Z_0 are the dissipation number and the line impedance constant, respectively, and are given by

$$D_n = \frac{4l\nu}{cd^2}, \tag{5}$$

$$Z_0 = \frac{4\rho c}{\pi d^2}, \tag{6}$$

where c is the speed of sound in the oil,

$$c = \sqrt{\frac{\beta_e}{\rho}}. \tag{7}$$

The three causal functions $1/\cosh\Gamma(s)$, $Z_c(s)\sinh\Gamma(s)/\cosh\Gamma(s)$, and $\sinh\Gamma(s)/Z_c(s)\cosh\Gamma(s)$ can be represented as infinite sums of quadratic modal transfer functions. The goal is to use a finite number of modes to approximate the otherwise infinite sum of the modal contributions for the outputs. Of particular interest for the time domain models sought in this paper is the state space formulation [10,15],

$$\begin{bmatrix}\dot{p}_{di}\\ \dot{q}_{ui}\end{bmatrix} = \begin{bmatrix} 0 & (-1)^{i+1}Z_0\omega_{ci} \\ -\dfrac{(-1)^{i+1}\omega_{ci}}{Z_0\alpha^2} & -\dfrac{32\nu\beta}{d^2\alpha}\end{bmatrix}\begin{bmatrix}p_{di}\\ q_{ui}\end{bmatrix} + \begin{bmatrix} 0 & -\dfrac{8\nu Z_0}{d^2 D_n} \\ \dfrac{8\nu}{d^2 Z_0 D_n \alpha^2} & 0\end{bmatrix}\begin{bmatrix}p_u\\ q_d\end{bmatrix},$$

$$i = 1,2,3...n. \tag{8}$$

The ω_{ci} are the modal undamped natural frequencies of blocked line for the linear friction model given by

$$\omega_{ci} = \frac{4\nu\pi\left(i-\frac{1}{2}\right)}{d^2 D_n}, \quad i = 1,2,3,...n. \tag{9}$$

The modification factors α and β are given as functions of the dimensionless modal frequencies $d^2\omega_{ci}/4\nu$ [10]. The output is the sum of the modal contributions and is expressed as

$$\begin{bmatrix}p_d\\ q_u\end{bmatrix} = \begin{bmatrix}\sum_{i=1}^{n} p_{di}\\ \sum_{i=1}^{n} q_{ui}\end{bmatrix} = [I_2 \;\; I_2 \cdots I_2] \times [p_{d1} \;\; q_{u1} \;\; p_{d2} \;\; q_{u2} \cdots p_{dn} \;\; q_{un}]. \tag{10}$$

It should be noted that the truncation to finite number of modes will introduce steady-state errors. Some methods have been suggested to recover the steady-state output based on the fact that at steady state the original four-pole equation, Eq. (2), reduces to

$$\begin{bmatrix}p_d\\ q_u\end{bmatrix}_{ss} = \begin{bmatrix}1 & -8D_n\\ 0 & 1\end{bmatrix}\begin{bmatrix}p_u\\ q_d\end{bmatrix}_{ss}. \tag{11}$$

Hsue and Hullender [16] discussed rescaling the truncated sum of the modal approximation for the dissipative model by its zero-frequency magnitude to bring about Eq. (11). Van Schothorst [9] and Hullender *et al.* [15] described an additive approach where the steady-state error is eliminated by adding a corrective feed-through term on the output equation (10). However, the transfer functions so implemented will no longer be strictly proper. This may entail the need for off-line algebraic manipulations when the transmission line is connected to static source and/or load linear resistances or other transmission line models with their own direct feed-through gains. The eigenvalues of the coupled system may then be altered by the steady-state correction [15].

Yang and Tobler [10] introduced methods that modify the input-matrix or use a state similarity transformation matrix to affect the steady-state correction while preserving the modal eigenvalues of the truncated model. Since comparable results are obtained by the use of either method, we adopt the input-matrix modification method here. Suppose matrices A_i and B_i represent, respectively, the feedback and input matrices in the modal state space Eq. (8). Introducing the input-matrix modifier G,

$$\begin{bmatrix}\dot{p}_{di}\\ \dot{q}_{ui}\end{bmatrix} = A_i\begin{bmatrix}p_{di}\\ q_{ui}\end{bmatrix} + B_i G\begin{bmatrix}p_u\\ q_d\end{bmatrix}. \tag{12}$$

The steady-state value of the n-mode approximation is then

$$\begin{bmatrix} p_d \\ q_u \end{bmatrix}_{ss} = \sum_{i=1}^{n} \begin{bmatrix} p_{di} \\ q_{ui} \end{bmatrix}_{ss} = -\sum_{i=1}^{n} (A_i^{-1}B_i)G \begin{bmatrix} p_u \\ q_d \end{bmatrix}_{ss}. \tag{13}$$

Comparing with the desired steady-state value given by Eq. (11) and solving for G,

$$G = -\left(\sum_{i=1}^{n} A_i^{-1}B_i \right)^{-1} \begin{bmatrix} 1 & -8Z_0D_n \\ 0 & 1 \end{bmatrix}. \tag{14}$$

The number of modes n to be chosen depends on the frequency range of interest for the application.

Similarly, for the return line from the servovalve, we can define the flow rate at the servovalve end and the pressure at the downstream (toward the tank) end as inputs to the model of the return line based on the other four-pole equation of causality dual to Eq. (2) [6]. Equally, we can use the observation that switching the sign convention of the flow direction for just the return line and using the four-pole equation dual to Eq. (2) yields the same set of four-pole equations as Eq. (2), provided the inputs to the model remain flow rate toward the servovalve end and pressure at the other end. This fact can easily be shown mathematically, but we omit it here for brevity and state that for the return line model all of the derivations presented above for modeling the supply line hold. The caveat is to exercise care in using the proper signs for the input and output flow rates at both ends of the return line when forming interconnections with other system components.

For step response simulations, it is desirable to have good estimates of the initial conditions of the modal states, especially when the interconnected system model contains nonlinearities. Usually, for a single pipeline section, the derivative of the modal output can be assumed to be zero just before the application of the step change in the input, and modal initial conditions can be computed from

$$\begin{bmatrix} p_{di}(0^-) \\ q_{ui}(0^-) \end{bmatrix} = -A_i^{-1}B_iG \begin{bmatrix} p_u(0^-) \\ q_d(0^-) \end{bmatrix}, \tag{15}$$

where the $[p_u(0^-), q_d(0^-)]^{\mathrm{T}}$ are the inputs just before the step change. For an interconnected pipeline system, the inputs to one pipeline section may be outputs of another section, in which case the determination of proper initial values for the modal states of each section can be done by trial and error. The step disturbances can also be applied after initial transients have died down. In general ''steady'' simulations, like those involving sinusoidal fatigue test wave forms, the modal initial conditions of the interconnected system are less important.

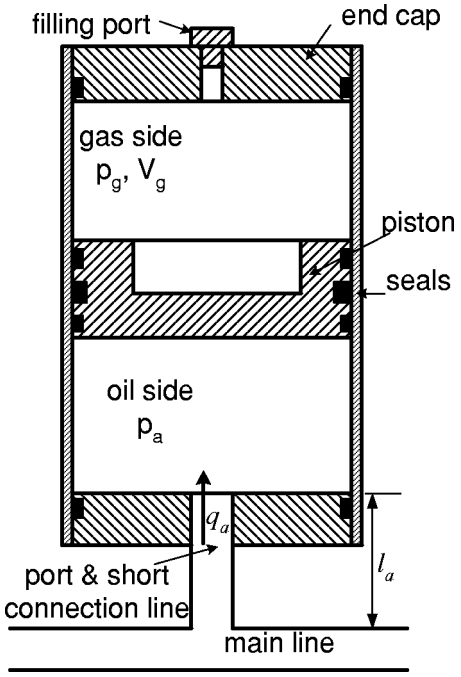

Fig. 4. Piston accumulator.

As shown in Fig. 3, the model described in this section requires few parameters to set up and simulate each transmission line section using linear state space models in the time domain. This is particularly more convenient than finite difference approaches, which may require rigorous descretization methods.

4. Modeling accumulators

For the nitrogen gas-charged accumulators, which are of piston type for our system (Fig. 4), we assume that the piston mass and seal friction are negligible. Under this assumption, the gas pressure and the oil pressure are equal. We also neglect the compressibility of the oil volume in the accumulator compared to the compressibility of the gas. Furthermore, we consider the gas to undergo a polytropic expansion and compression process with polytropic exponent m.

$$p_g V_g^m = \text{const.} \tag{16}$$

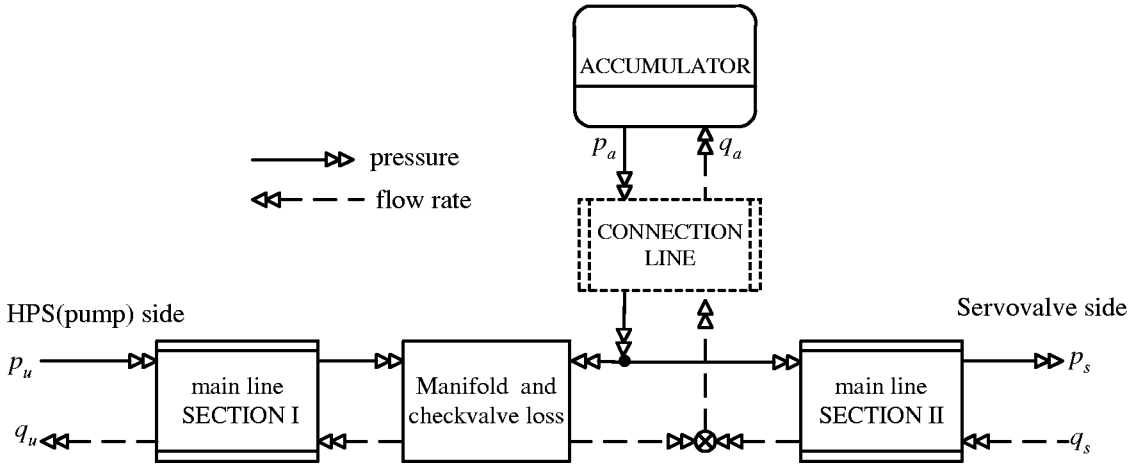

Fig. 5. Model interconnections for the supply line (Version I).

The exponent m approaches 1 for a slow (nearly isothermal) process and the specific heat ratio of the gas for a rapid (adiabatic) process on an ideal gas. However, it should be noted that if heat transfer effects were to be included, then real gas equations of state should be used together with appropriate energy conservation laws. For the work presented here, the present model was found to be sufficiently accurate.

Given initial gas pressure p_{g0} and gas volume, V_{g0}, the gas pressure is computed from Eq. (16), which is equivalent to

$$\dot{p}_g = \frac{m p_g}{V_{g0} - \int_0^t q_a dt} q_a, \quad p_g(0) = p_{g0}, \quad (17)$$

where q_a is the flow rate of the hydraulic oil to the accumulator. For simulations involving disturbances applied at the servovalve, it is reasonable to assume that the accumulator already develops an initial gas pressure through a slow isothermal process[1] $(m=1)$. The initial gas volume V_{g0} can be estimated by applying Eq. (16) between the pre-charge state (the gas pre-charge pressure at accumulator capacity) and the initial state at the onset of the disturbance. The initial gas pressure p_{g0} can be estimated as the HSM pressure minus the pressure drop in the connection lines.

5. Model interconnections for the supply line

The components on the supply line of the simplified model shown in Fig. 2 can be interconnected as shown in Figs. 5 or 6. The arrows indicate the input-output causality assigned for each subsystem. Each of the blocks section I and section II implement Eqs. (8)–(14) for the corresponding sections of the supply line.

Integration causality is the desired form for the model of the accumulator, which is given by Eq. (17). It was pointed out by Viersma [7] that the flow dynamics in the short branch-away connection lines to the accumulators are significant in most cases. Under the linear resistance assumption given by Eq. (1), the subsystem ''manifold and check valve loss'' can be configured either as a pressure-input/flow rate-output subsystem (in version I, Fig. 5) or as a pressure-input/pressure-output subsystem (in version II, Fig. 6). As a consequence, the model of the short accumulator connection line changes between version I and version II. The model of the short connection line in version I has the same structure as the one described above for the sections of the main supply line. The model for the short connection line in version II is derived using the modal approximation for the relevant four-pole equations with (p_u, p_d) as input and (q_u, q_d) as output, as de-

[1]The present system has an additional slow turn-on/turn-off accumulator that enables the HSM to come to full system pressure from an off state in a slow and controlled manner. The servovalve disturbances considered in this study are applied after the whole system has reached normal operating conditions.

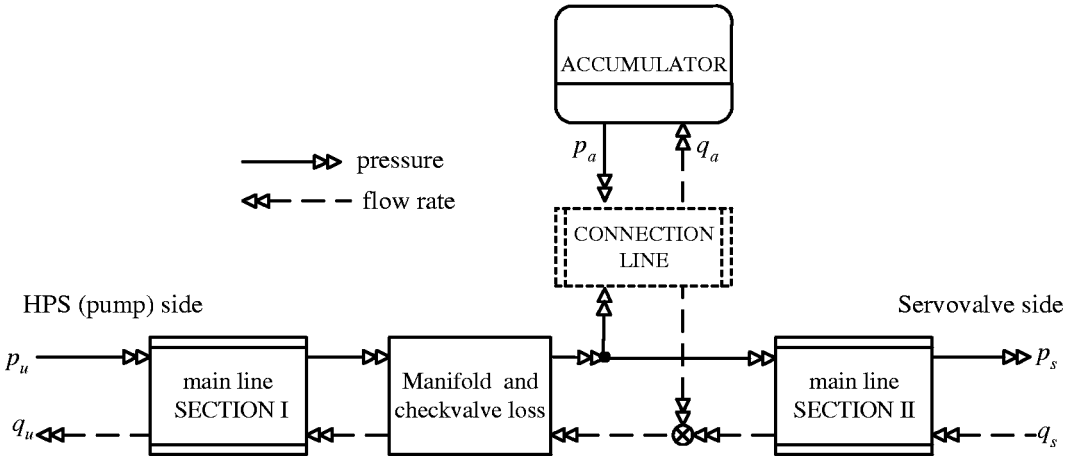

Fig. 6. Model interconnections for the supply line (Version II).

scribed by Ayalew and Kulakowski [14]. It was shown there that the dynamics of the short connection line can be approximated by a first-order term that reduces to a series interconnection of hydraulic resistance and inertance. This result goes along with the convenient assumption that the oil side compressibility in the accumulator is negligible compared to that of the gas side. This result also makes version II preferable to version I, since it reduces the order of the overall system and verifies a physically supported model order reduction.

The model for the return line is developed in a similar way noting the reverse direction of the flow, as mentioned earlier. It should be noted that the modularity of the subsystem model interconnections allows changes to be made to the system model with ease.

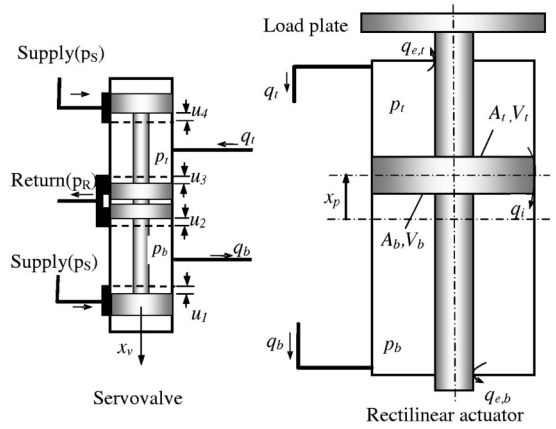

Fig. 7. Schematic of a rectilinear actuator and servovalve.

6. Model for servovalve and actuator

Physical models of electrohydraulic servoactuators are quite widely available in the literature [1–4,7,9,17]. The model presented here is adapted to apply to a four-way servovalve close coupled with a double-ended piston actuator.

Fig. 7 shows a double-ended translational piston actuator with hydraulic flow rates q_t from the top chamber and q_b to the bottom chamber of the cylinder. Leakage flow between the two chambers is either internal (q_i) between the two chambers or external from the top chamber $(q_{e,t})$ and from the bottom chamber $(q_{e,b})$. A_t and A_b represent the effective piston areas of the top and bottom face, respectively. V_t and V_b are the volumes of oil in the top and bottom chamber of the cylinder, respectively, corresponding to the center position $(x_p = 0)$ of the piston. These volumes are also considered to include the respective volumes of oil in the pipelines between the close-coupled servovalve and actuator as well as the small volumes in the servovalve itself.

We assume that the pressure dynamics in the lines between the servovalve and the actuator are negligible due to the close coupling.[2] Furthermore, even for a long-stroke actuator used in a flight simulator application, Van Schothorst [9] has

[2]This is to say that any resonances introduced by the short-length lines are well above the frequency range of interest for our system. In fact, this can be verified using the model development presented earlier or referring to the results of Van Schothorst [9].

shown that the pressure dynamics in the actuator chambers need not be modeled using distributed parameter models. It is therefore assumed that the pressure is uniform in each cylinder chamber and is the same as the pressure at the respective port of the servovalve.

Starting with the continuity equation and introducing the state equation with the effective bulk modulus for the cylinder chambers, it can be shown that the pressure dynamics are given by (see, for example Ref. [2])

$$\frac{dp_b}{dt}=\frac{\beta_c}{V_b+A_b x_p}(q_b-A_b\dot{x}_p+q_i-q_{e,b}), \tag{17a}$$

$$\frac{dp_t}{dt}=\frac{\beta_c}{V_t-A_t x_p}(-q_t+A_t\dot{x}_p-q_i-q_{e,t}). \tag{17b}$$

These equations show that the hydraulic capacitance, and hence the pressure evolution in the two chambers, depends on the piston position. The leakage flows q_i, $q_{e,b}$, and $q_{e,t}$ are considered negligible.

The predominantly turbulent flows through the sharp-edged control orifices of a spool valve, to and from the two sides of the cylinder chambers, are modeled by nonlinear expressions [1,2,4]. Assuming positive flow directions as shown in Fig. 7, we have

$$q_b=K_{v,1}sg(x_v+u_1)\mathrm{sgn}(p_S-p_b)\sqrt{|p_S-p_b|} - K_{v,2}sg(-x_v+u_2)\mathrm{sgn}(p_b-p_R)\sqrt{|p_b-p_R|}, \tag{18a}$$

$$q_t=K_{v,3}sg(x_v+u_3)\mathrm{sgn}(p_t-p_R)\sqrt{|p_t-p_R|} - K_{v,4}sg(-x_v+u_4)\mathrm{sgn}(p_S-p_t)\sqrt{|p_S-p_t|}, \tag{18b}$$

where the $sg(x)$ function is defined by

$$sg(x)=\begin{cases}x, & x\geqslant 0\\ 0, & x<0\end{cases}. \tag{19}$$

The parameters u_1, u_2, u_3, u_4 are included to account for valve spool lap conditions as shown in Fig. 7. Negative values represent overlap while positive values represent underlap. The valve coefficients $K_{v,i}$ are given by

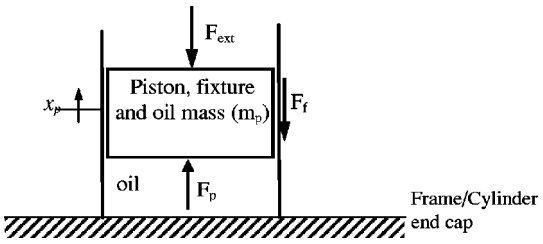

Fig. 8. Actuator with a simple load model.

$$K_{v,i}=c_{d,i}w_i\sqrt{2/\rho}, \quad i=1,2,3,4. \tag{20}$$

These coefficients could be computed from data for the discharge coefficient $c_{d,i}$, port widths w_i, and oil density ρ. If we assume that all orifices are identical with the same coefficient K_v, then the value of K_v can also be estimated from manufacturer data for the rated valve pressure drop (Δp_N), rated flow (Q_N), and maximum valve stroke ($x_{v\,\max}$) using the following equation [1,4]:

$$K_{v,i}=K_v=\frac{Q_N}{x_{v\,\max}\sqrt{1/2\Delta p_N}}, \quad i=1,2,3,4. \tag{21}$$

As an approximation of the servovalve spool dynamics, a second-order transfer function or equivalently a second-order state space was extracted from manufacturer specifications,

$$\frac{X_v(s)}{I_v(s)}=\frac{G_v\omega_{n,v}^2}{s^2+2\zeta_v\omega_{n,v}s+\omega_{n,v}^2}. \tag{22}$$

The state equations governing piston motion are derived considering the loading model for the actuator. For the test system, the actuator cylinder is rigidly mounted on a load frame, which we use as an inertial frame as shown in Fig. 8.

The upward force on the actuator piston due to the oil pressure in the two cylinder chambers is given by

$$F_p=A_b p_b-A_t p_t. \tag{23}$$

The friction force on the piston in the cylinder is denoted by F_f and the external loading including specimen damping and stiffness forces are lumped together in F_{ext}. The equations of motion are easily derived by applying Newton's second law:

$$\dot{x}_p=v_p, \tag{24}$$

$$\dot{v}_p = \frac{1}{m_p}[A_b p_b - A_t p_t - F_{ext} - F_f - m_p g]. \tag{25}$$

Eqs. (17a), (17b), (24), and (25) with q_b and q_t given by Eqs. (18a) and (18b) constitute the state space model for the servovalve and loaded actuator subsystem under consideration. These equations also contain the major nonlinearities in the system: the variable capacitance and the square root flow rate versus pressure drop relations. Nonlinearity is also introduced in Eq. (25) by the nonlinear friction force, which includes Coulomb, static, and viscous components [1,18] as discussed next.

7. Modeling and identification of friction

Friction affects the dynamics of the electrohydraulic servovalve as well as the dynamics of the actuator piston. Friction in the servovalve is generally considered to be of Coulomb type acting on the spool of the valve and can in practice be sufficiently eliminated by using dither signals [9]. The particular friction effect of interest in this section is the model of the frictional forces that appear in the equations of motion of the actuator piston. The literature offers various empirical models applied to specific hydraulic actuators [1,3,18,19]. In the most general case, friction in the actuator cylinder is considered to be a function of the position and velocity of the piston, the chamber pressures (the differential pressures when the piston is sticking near zero velocity), the local oil temperature and also running time.

In this study, open-loop and closed-loop tests were performed to identify the friction force on the actuator piston by assuming it to be a function of velocity. Open-loop tests involved changing the set current input to the servovalve while measuring the steady-state piston velocity and cylinder chamber pressure responses. The system behaves as a velocity source in the open loop. The closed-loop test involved tracking a 2-Hz 35-mm sine wave piston position command under P control while measuring acceleration, velocity, and chamber pressures. In both the open-loop and closed-loop tests, the friction is then estimated using Newton's second law. Fig. 9 shows the result of multiple open-loop tests and a closed-loop test. The closed-loop test clearly shows the hysteretic

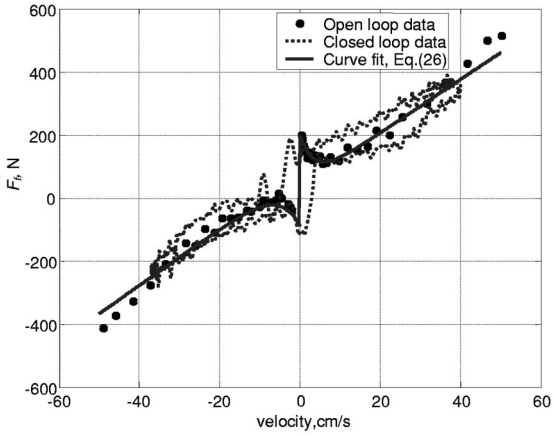

Fig. 9. Piston friction force.

behavior of friction. For simplicity, we use the common memory-less analytical model of friction (without hysteresis) as a function of velocity, given by Eq. (26) and included in Fig. 9,

$$F_f = F_v^{\pm}\dot{x}_p + \mathrm{sgn}(\dot{x}_p)(F_c^{\pm} + (F_s^{\pm} - F_c^{\pm})e^{(\dot{x}_p/C_s)}). \tag{26}$$

The asymmetry of the friction force with respect to the sign of the velocity observed in the measured data is taken into account by taking different coefficients in Eq. (26) for the up and down motions. The strong scatter in the estimation data is typical of friction phenomena.

8. Experimental validation of the model

The model described in the previous sections was implemented in MATLAB/SIMULINK, and baseline open-loop and closed-loop experiments were conducted to validate it. In these experiments, a simple load mass is rigidly attached to the piston rod. For the models of each of the sections of the supply and return line hoses, only six modes are retained in the modal approximation. This was decided considering the actuator hydraulic natural frequency of 172 Hz computed using formulas from linear models (see Merritt [4]) and selecting the natural frequency of the highest mode of the approximation for each section to be close to twice this value. From manufacturer frequency response data for the servovalve, the natural frequency for the servovalve was estimated to be 140 Hz with a damping ratio of 1.

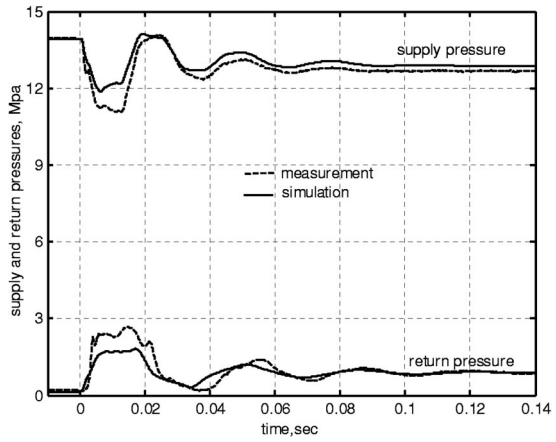

Fig. 10. Supply and return pressure following a step change in servovalve current.

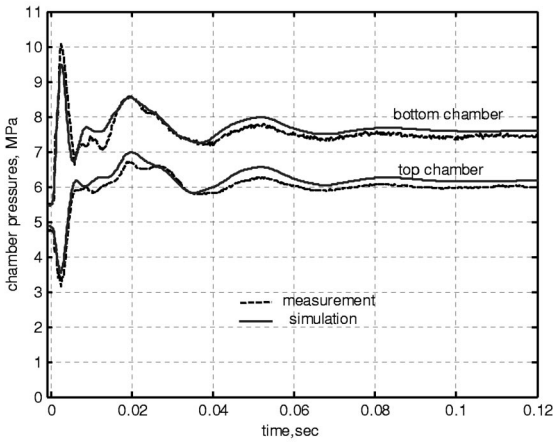

Fig. 11. Open-loop cylinder chamber pressure responses.

To measure the supply and return pressure fluctuation, pressure transducers were mounted on the supply and return ports at the servovalve and a 50-mA rated step current was supplied to the servovalve in the open-loop. Fig. 10 shows a comparison of the supply and return pressure from measurement and simulation. Two observations can be made from this figure. First, the supply and return pressure fluctuations contain the fundamental periods of 25 and 32 ms, respectively. These correspond to fundamental frequencies of about 40 and 31 Hz, respectively. The implication of these fluctuations is that the bandwidth of the actuator is limited by the dynamics of the supply and return hoses, since the other dynamic elements including the servovalve and the actuator have higher corner frequencies. Second, the model follows the measurement well. In particular, the frequency contents match nicely. The discrepancies can be attributed to errors in the estimation of effective bulk moduli for the different hose sections, and the estimation of manifold pressure drops as well as unknown but estimated parameters in the adopted simplified model of the servovalve.

The open-loop response of the system can be investigated further by looking at the cylinder chamber pressures shown in Fig. 11 and the piston velocity response shown in Fig. 12 following the same step-rated current input to the servovalve. It can be seen from Fig. 11 that the simulation predictions of chamber pressures follow the measurements and that the supply and return pressure dynamics introduced by the long sections of hoses are reflected in the individual cylinder chamber pressures.

In the open-loop piston velocity response shown in Fig. 12, the velocity signal was obtained by low-pass filtering and differentiating the LVDT position signal. The figure shows that the model does a fairly good job of predicting the piston velocity response as well. The differences are again attributed to uncertainties in the servovalve model and also errors in friction estimation, which has a considerable scatter, as shown in Fig. 9.

9. Predicting system performance

It should be recalled that, for the present system, the fundamental frequencies of oscillation of the

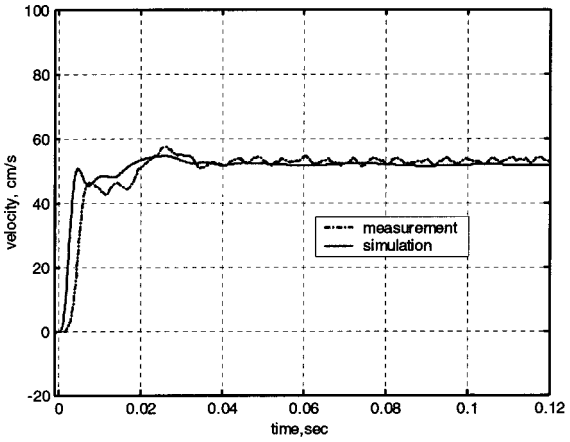

Fig. 12. Open-loop piston velocity response.

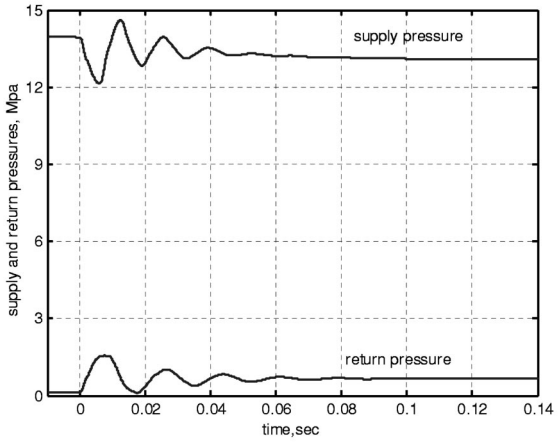

Fig. 13. Supply and return pressures with 1.524-m-long lines.

supply and return line pressures are lower than the natural frequencies of both the actuator and the servovalve. This implies that the bandwidth of the test system is limited by supply and return line dynamics. The model described in this paper was used to predict pressure fluctuations in the supply and return lines by running simulations for contemplated modifications to the layout of the test system. In particular, it was desired to see if reducing the lengths of sections II of both the supply and return hoses in the layout (Fig. 2) produces significant changes in the supply and return line pressure dynamics at the servovalve. The lengths of sections I were kept unchanged since the physical constraints of housing the HPS required about 3.048 m of hose lengths for sections I of both the supply and return lines. The goal of the study was to see if actually there will be significant gains from these measures in terms of increasing the effective bandwidth for the actuator.

As a first case, the hoses of sections II were reduced to half the original length of 3.048 m. A length of 1.524 m was considered sufficient to still place the HSM unit on the ground while the actuator was mounted on the load frame. Fig. 13 shows the supply and return line pressures at the servovalve following the open-loop test described previously with the lengths now at 1.524 m.

It can be seen from Fig. 13 that the fundamental period of pressure fluctuation shifts to 13.3 and 18.5 ms, respectively, for the supply and return lines. These correspond to fundamental frequencies of 75 Hz on the supply line and 54 Hz on the return line. The settling times are reduced by about 20 ms or about 22% compared to the original setup with 3.048 m lengths of sections II of the supply and return line hoses. The peak amplitude of the oscillation is also slightly reduced, as shown in Table 1. The bandwidth of the hydraulic actuator can therefore be expected to be improved accordingly. However, the accumulators were not shown to be effective in filtering the fluctuations completely.

Table 1
Summary of step response simulation results.

Lengths of sections II (m)	Fundamental frequency of oscillation in step response (Hz)		Peak amplitude of oscillation (Mpa)	
	Supply pressure	Return pressure	Supply pressure	Return pressure
3.048	40	31	1	0.94
2.286	49	39	0.97	0.91
1.524	76	57	0.94	0.88
0.7512	147	115	0.87	0.71
0	N/A	N/A	0.0	0.0

As a second case, the sections II of the hoses are considered to be removed from the system and by so doing the HSM is close-coupled with the actuator. This consideration would need significant changes to the physical design of the load frame to allow the HSM to be mounted on it together with the actuator. In the model, the corresponding sub-

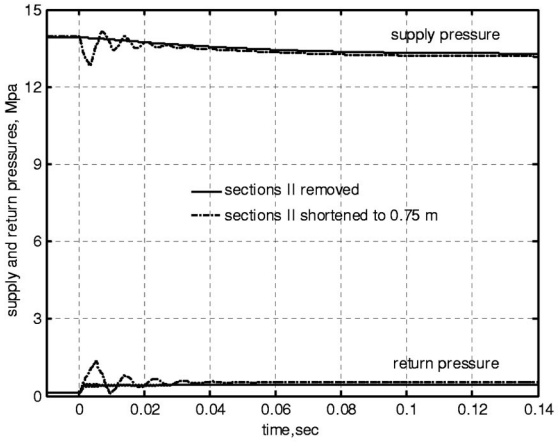

Fig. 14. Supply and return pressures with close-coupled HSM and shorter lines.

system of section II was removed from the schematic in Fig. 6. Fig. 14 shows simulation results for this case as well as a hypothetical case for which the hoses are shortened further to 0.7512 m. It can be seen that the effect of the accumulators in filtering out the dynamics of the sections I from the supply and return lines is particularly evident in the close-coupled HSM case. In addition, the steady-state pressure drops in the supply and return line are smaller in this case compared to the original setup (Fig. 10) and to the case with 1.524-m lengths for sections II (Fig. 13). The improvements predicted by the case of lengths 1.524 and 0.7512 m seem rather small compared to the case of close coupling the HSM with the actuator.

Table 1 summarizes these results, including one more additional length for sections II. It can be seen that the peak amplitudes of the supply and return pressure oscillations are progressively reduced as the length of the hoses becomes shorter while the fundamental frequency of the oscillations for the step responses becomes larger. In the limit case of 0-m length for sections II, which means the HSM accumulators are close coupled with the servovalve, the oscillations are eliminated. In this case, the accumulators effectively suppress the oscillations arising out of the sections I of the supply and return line hoses.

10. Conclusions

In this paper, a model of an electrohydraulic actuator system focusing on supply and return line dynamics was presented. A model of hydraulic transmission lines based on modal approximation techniques was adopted yielding state space descriptions suitable for time domain simulations. The interconnection model of the electrohydraulic system developed here is an attractive simulation tool for the following reasons.

1. The distributed parameter transmission line model requires only aggregate line parameters such as line length, diameter, and effective bulk modulus in state space dynamic models. It therefore enables a quick investigation of line effects in a time domain analysis. It was used here to model hydraulic hoses with experimental validation.

2. The time domain simulation, in turn, makes it possible to include nonlinear actuator models. This is particularly useful for the study of actuator models with linear and nonlinear control systems without ignoring supply and return line pressure variations introduced by transmission line dynamics.

3. The model of the overall hydraulic system was modular. Subsystem models can easily be changed for desired emphasis observing only the input-output causality. For example, a detailed model of the servovalve can be used in place of the simplified model used in this paper, thereby improving the predictive power of the overall model.

Simulation results for some open-loop step responses were compared against experimental results for the test system. It is felt that the model performs well, given the minimal amount of information it uses to enable a time domain simulation. The use of constant bulk modulus values for the hose material, which in reality depends on pressure and frequency, may explain some of the difference between the simulation and measurement. A more detailed servovalve model with measured operating characteristics, instead of the rated specifications, could also improve the accuracy of the overall electrohydraulic system model presented here.

A simulation analysis of the effects of the lengths of sections of the supply and return lines between the HSM accumulators and the servovalve was done. It was concluded that reducing the lengths of these lines progressively reduces the supply and return pressure fluctuation at the servovalve during dynamic excursions by the actuator. The test system bandwidth was correspondingly improved. The best scenario was shown to be one where the accumulators were close coupled with the servovalve, thereby employing the accumulators effectively in filtering out the effects of the sections of the supply and return lines between the pump (HPS) and the accumulators.

In conclusion, it is recommended that hydraulic control system design and analysis include the modeling approach presented here, to account for the effects of supply and return line dynamics rather than assuming constant values for the supply and return pressure as has been usually done in the literature. It was also demonstrated that the approach could be used to make a quick assessment of alternative layouts for supply and return lines in terms of minimizing transmission line dynamics. The method can easily be adopted to other applications of hydraulic machinery and test sys-

tems where hydraulic oil supply and return lines of significant length are involved.

References

[1] Jelali, M. and Kroll, A., Hydraulic Servo-systems: Modelling, Identification and Control (Advances in Industrial Control). Springer-Verlag, London, 2003.

[2] Kugi, A., Non-linear Control Based on Physical Models, Lecture Notes in Control and Information Sciences No. 260. Springer-Verlag, London, 2001.

[3] Sohl, G. A. and Bobrow, J. E., Experiments and Simulations on the Nonlinear Control of a Hydraulic Servosystem. IEEE Trans. Control Syst. Technol. **7**(2), 238–247 (1999).

[4] Merritt, Herbert E., Hydraulic Control Systems. Wiley, New York, 1967.

[5] D'Souza, A. F. and Oldenburger, R., Dynamic response of fluid lines. J. Basic Eng. **86**(3), 589–598 (1964).

[6] Goodson, R. E. and Leonard, R. G., A survey of modeling techniques for fluid line transients. J. Basic Eng. **94**(2), 474–482 (1972).

[7] Viersma, T. J., Analysis, Synthesis and Design of Hydraulic Servosystems and Pipelines, Studies in Mechanical Engineering I. Elsevier Publishing Co., Amsterdam, the Netherlands, 1980.

[8] Woods, R. L., Hsu, C. H., and Chung, C. H., Comparison of theoretical and experimental fluid line responses with source and load impedance. Fluid Transmission Line Dynamics, edited by M. E. Franke and T. M. Drzewiecki. ASME Special Publications, New York, 1983, pp. 1–36.

[9] Van Schothorst, G., Modeling of Long-Stroke Hydraulic Servo-Systems for Flight Simulator Motion Control and System Design. Ph.D. thesis, Delft University of Technology, Delft, The Netherlands 1997.

[10] Yang, W. C. and Tobler, W. E., Dissipative modal approximation of fluid transmission lines using linear friction model. J. Dyn. Syst., Meas., Control **113**, 152–162 (March 1991).

[11] MTS Corporation, Hardware Product Manual, 290.1X, 290.2X, and 290.3X Hydraulic Service Manifold, 1985.

[12] Blackburn, J. F., Reethof, G., and Shearer, J. L., Fluid Power Control. MIT Press, Cambridge, MA, 1960.

[13] McCloy, D. and Martin, H. R., Control of Fluid Power: Analysis and Design, second edition. Halsted Press, Chichester, UK, 1980.

[14] Ayalew, B. and Kulakowski, B. T., Transactions of the ASME, Journal of Dynamic Systems, Measurement and Control (in press).

[15] Hullender, D. A., Woods, R. L., and Hsu, C.-H., Time domain simulation of fluid transmission lines using minimum order state variable models. Fluid Transmission Line Dynamics. ASME special publication, 1983, pp. 78–97.

[16] Hsue, C. Y.-Y. and Hullender, D. A., Modal approximations for the fluid dynamics of hydraulic and pneumatic transmission lines, Fluid Transmission Line Dynamics, edited by M. E. Franke and T. M. Drzewiecki. ASME special publication, 1983, pp. 51–77.

[17] Dransfield, P., Hydraulic Control Systems: Design and Analysis of their Dynamics, Springer-Verlag, Berlin, 1981.

[18] Alleyne, A. and Liu, R., A simplified approach to force control for electro-hydraulic systems. Control Eng. Pract. **8**, 1347–1356 (2000).

[19] Manhartsgruber, B., Singular perturbation analysis of an electrohydraulic servo-drive with discontinuous reduced dynamics. Proceedings of the 1999 ASME Design Engineering Technical Conference, Las Vegas, Nevada, 1999, pp. 2001–2011.

Beshahwired Ayalew was born in Goba, Ethiopia in 1975. He earned his BS degree in mechanical engineering from Addis Ababa University, Ethiopia and his MS degree, also in mechanical engineering, from the Pennsylvania State University, USA. He is currently a Ph.D. candidate in mechanical engineering at the Pennsylvania State University. His research interests include dynamic systems and control, energy systems, mechanical design, and vehicle dynamics.

Bohdan T. Kulakowski obtained his Ph.D. from the Polish Academy of Sciences in 1972. He has been with Penn State University since 1979, where he is currently a professor of mechanical engineering. Dr. Kulakowski teaches undergraduate and graduate courses on engineering measurements, system dynamics, and controls. He is a co-author of the book ''Dynamic Modeling and Control of Engineering Systems.'' Dr. Kulakowski is a Fellow of ASME. His research interests are in vehicle testing, vehicle dynamics, and vehicle interaction with environment.